

Reviewer's comment:

*The manuscript by Meler et al. investigated the size-fractionated absorption spectra of particles, phytoplankton, and non-algae particles (NAP) in the southern Baltic Sea. They also conducted the measurement of total and size-fractionated suspended particulate matter (SPM) and Chlorophyll (Chl) a concentrations and then examined the relationships between the absorption coefficients, SPM, and Chl a concentrations for each size fraction. They found that the SPM-specific absorption coefficients are a useful parameter to distinguish between large and small plus medium particle fractions. The data presented in this study is informative. However, this manuscript requires considerable alteration along the lines I have suggested below.*

Author's response:

We thank the Reviewer for insightful critical comments on our work.

We modified selected fragments of the text and figures, in accordance with most of the Reviewer's suggestions.

Reviewer's comment:

**Major comments**

*The description of total and size-fractionated Chl a-specific NAP absorption needs more detail. It is possible to understand the meaning for calculating the absorption coefficients of particles ( $a_p$ ) and phytoplankton ( $a_{ph}$ ) normalized by Chl a and SPM concentrations to see the contribution of each size component to the spectral shape and magnitude. However, I am not sure the significance of the Chl a-specific NAP absorption spectra and coefficient at 443 nm as shown in Figures 6a – e, and 9c, 10c.*

Author's response:

Figure 6 shows  $a_d(443)$  vs Chl a and vs SPM coefficients, while Figure 9c and 10c show chlorophyll-specific  $a_d(443)$ . In general, if we can express  $a_p$  and  $a_{ph}$  in the form of a Chl a-dependent function, then so can  $a_d$ , since  $a_p = a_d + a_{ph}$ . For clean ocean waters (the so-called Case1) Bricaud et al. (1998) presented Chl a-specific NAP absorption  $a_d(\text{Chl a})$  can be determined from the difference of  $a_p(\text{Chl a}) - a_{ph}(\text{Chl a})$  (Woźniak & Dera, 2007). In the case of the optically complex Baltic Sea, these relationships are not so simple, and we just wanted to illustrate what they look like. For the analyzed data set, on average, 52% of suspended matter was organic matter of both autogenic and allogenic origin, and the contribution of inorganic matter to light absorption is not significant (Woźniak and Dera, 2007). Therefore, the absolute values of  $a_d$  in the analyzed set depend on the concentration of organic matter suspended in the water, which is not phytoplankton. Chl a-specific NAP absorptions are independent of the SPM concentration, and their values and spectral distributions are determined by the absorption properties of the suspension particles themselves, i.e. they depend on the chemical and physical properties of the material they are made of (chemical composition, optical properties, sizes, shapes).

Earlier, we heard the opinion that the concept of  $a_{\text{NAP}}$ , or "particles other than algae", is too empirical, because it consists of an unknown admixture of mineral and organic detritus. The very different refractive indices of mineral and organic matter make it impossible to interpret changes in  $a_{\text{NAP}}$  in any quantitative way. Mass-specific  $a_{\text{NAP}}$  based on SPM are of no value without the partitioning of SPM into PIM and POM (Duarte et al. 1998, Richter and Stavn,

2014). On the other hand, chlorophyll-specific  $a_{\text{NAP}}$  may be of some value. Therefore, in our work we decided to show both approaches.

Reviewer's comment:

*I agree with the author's assertion that the data obtained by this study could improve the model to retrieve the inherent optical properties (IOPs) in the Baltic Sea (Lines 464 – 465). However, it is not clear that which of the results or relationships examined in this study would contribute to the improvement of the IOPs models and how to expand the results into the models for estimating the size parameters. Given that many cases have already been reported in the literature (as cited by the authors themselves in the Conclusion section), it would be advisable to explain specific information on the improvement of IOP models.*

Author's response:

Our research results are preliminary and very limited.

The analyzes presented by us are an introduction to further research, in which HPLC data and the actual particle size distribution should be taken into account in order to formulate an absorption model for particles in different size classes, similarly to Devred et al. (2006, 2011) and Brewin et al. (2010, 2011).

Our pilot studies on the study of the contribution of individual particle size fractions in the total SPM, Chla and related absorption properties for the southern part of the Baltic Sea indicate the need to develop this topic, especially for the remote estimation of the size structure of phytoplankton populations, the so-called PFT.

These sentences have been included in Conclusions.

Reviewer's comments:

*The large part of the sentences in the Introduction reviews the previous literatures. Therefore, it seems to me that it is hard from reading the Introduction to understand why this study is needed. To better organized the introduction and objectives, I would encourage the authors to rewrite the section. Similarly, abstract and most parts of results and discussion sections, especially 3.2, 3.3, and 3.4, are not well organized. It is descriptive and is like a data report, making difficult to follow what is the new findings described in this study. However, I believe that the authors can elaborate.*

Reviewer's comments:

*Figure 2a showed the results of size-fractionated "SPM" in each sampling station. A more appropriate legend would be required for Figure 2a to better reflect the investigation of SPM.*

Author's response:

We agree with the opinion of the Reviewer. Sections Introduction, 3.2, 3.3, 3.4 have been modified. Figures and tables have been modified. The descriptions were extended with the seasonal and spatial division of the analyzed data set.

In the Introduction section, we have completed the goals of our research.

Various approaches to identify the size structure of phytoplankton populations from satellite data are detailed in the IOCCG report (2014), which describes the possibilities of developing algorithms for remote determination of the contribution of various functional types of phytoplankton (PFT) included in the total population in the waters under study. The PFT concept is used in the study of a number of ecological and biogeochemical problems, especially in model studies. A specific functional type may represent a group of different species related to each other due to certain distinguished features. This approach is of growing interest as it allows for a more thorough study of the role of phytoplankton in global sea and ocean cycles involving the circulation of major chemical elements such as carbon, nitrogen, sulfur and iron, as well as photosynthesis and primary production.

The above mentioned methods of estimating the contribution of phytoplankton size classes do not work for the Baltic Sea, which is a reservoir classified as optically complex (for the DPA method, the results are presented in Meler et al., 2020).

(...)

For this purpose, *in situ* studies should be carried out, which would allow to directly determine the light absorption coefficients not only by phytoplankton, but also by all particles and detritus in various size fractions. The research described in this paper is in line with the objectives and guidelines of the Monitoring and Evaluation Strategy of the Helsinki Commission (HELCOM), which aims to ensure the evaluation and monitoring of data that can be used by HELCOM, both for international and national monitoring. The strategy is designed to ensure data production and dissemination by contracting parties of EU Member States. These countries are obliged to comply with several EU directives, such as the Marine Strategy Framework Directive (MSFD), the Water Framework Directive (WFD), the Habitats and Birds Directives, the EU Strategy for the Baltic Sea Region (EUSBSR) and the EU Integrated Maritime Policy (HELCOM, 2013). First of all, the Strategy aims to support ecosystem-based maritime spatial planning (MSP) in the Baltic Sea based on ecosystem. It is done by enabling high-quality spatial data and assessment tools for MSP purposes.

Our research may be useful in examining whether the use of SPM and Chl<sub>a</sub> data from MERIS or other optical sensors installed on satellites (e.g. OLCI - Ocean and Land Color Instrument) can be used as "high-quality spatial data" and as a HELCOM regional assessment tool.

We have shown in Figures 2-3 and 5-8, the division into seasons and sampling areas. And the relevant comments are placed in the text of manuscript.

New Figure 2

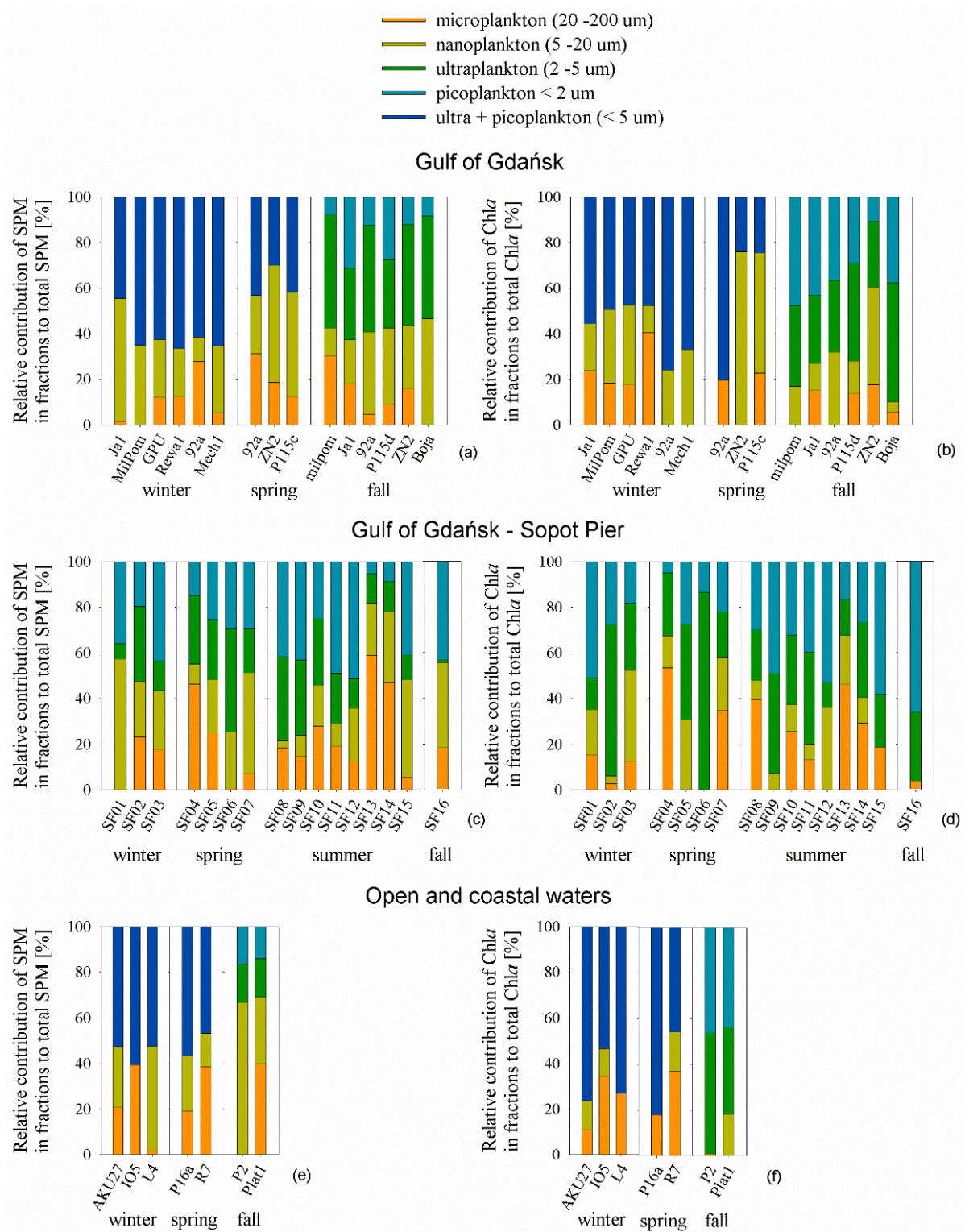


**Figure 2: Relative contribution of SPM in the selected fraction to the total SPM – left panel (a, c, e), and Chl<sub>a</sub> in the selected fractions to the total Chl<sub>a</sub> – right panel (b, d, f), divided due to region (Gulf of Gdańsk, Sopot Pier, Open and coastal waters) and seasons**

In winter, when there is minimal biological activity in the Baltic Sea, it can be seen that the largest contribution in SPM (> 50%) had particles < 5 μm, which can be seen in both GG and

OCW. In the spring, this trend continued in OCW, while the contribution of micro and nano particles increased in GG. In the autumn period, particles  $< 5 \mu\text{m}$  again had the largest contribution in the GG, with a predominance of ultra particles. In the case of OCW, the contribution of small particles decreased and nano and micro particles ( $> 5 \mu\text{m}$ )  $> 60\%$  dominated. The Sopot Pier dataset shows temporary variability over 10 months and is the only one that takes into account the summer season. It can be seen that in most cases, in winter, spring and autumn, the contribution of small ( $< 5 \mu\text{m}$ ) and medium and large ( $> 5 \mu\text{m}$ ) particles in the SPM is comparable, except for SF06. In summer (SF08-SF12 and SF15) particles  $< 5 \mu\text{m}$  contributed the most to SPM, with pico particles predominating, only during phytoplankton blooms, where large algae gathered at the beach, samples were dominated by micro particles, and the proportion of small particles was below 20 %.

The right panel of Figure 2 shows the proportion of Chl *a* in individual size fractions.

The average contribution of chlorophyll *a* in a given size class to the total concentration of Chl *a* for all data is the highest for pico-particles (35 %) and ultra-particles (35 %), while the average contribution of Chl *a* in nano and micro-particle classes is about 15 % each. The range of variability of the contributions of individual size classes in the total Chl *a* changed as follows: micro-particles from 0 to 53 %, nano particles from 0 to 76 %, ultra-particles from 11 to 86 % and pico-particles from 5 to 66 %. (second part of Table 2). In the GG in the winter, Chl *a* in the ultra+pico particles class had about 50% share, the rest was for medium and large particles, and it can be seen that despite the small contribution of micro-particles in SPM, the proportion of Chl *a* in this size class was about 20% for stations Ja1, Milpom and GPU, and for Rewa1 about 40% (probably the particles lifted from the bottom contained a lot of organic detritus). In turn, for example, for station 92a, the contribution of micro-particles was about 30%, and the proportion of Chl *a* for the same station is close to zero, which means that these particles were inorganic. In autumn, the contribution of Chl *a* for particles  $< 5 \mu\text{m}$  (except for the ZN2 station located closest to the mouth of the Vistula River) was on average about 80%. In the case of OCW waters, an average of  $> 60\%$  of Chl *a* in the classes of small particles and about 20% of micro-particles was observed in winter and spring. In autumn, small particles accounted for more than 80% of Chl *a* in OCW waters. The micro and nano particles in these waters were mostly inorganic. This also results from SPM analyses. At the Plat1 station, no Chl *a* contribution was observed for the micro particle class and  $< 20\%$  Chl *a* contribution in the nano-particle fraction. At the Sopot Pier station, the proportion of Chl *a* in the classes of small particles,  $< 5 \mu\text{m}$ , in winter was  $> 60\%$  with a maximum value of 95% observed on SF02. In the spring, the contribution of Chl *a* in the class of small particles for SF04 and SF07 was about 30%, for SF05 about 65%, and for SF06 100%. In the summer season, the contribution of small particles  $< 5 \mu\text{m}$  was still dominant, except for experiments SF13 and SF14, during which phytoplankton blooms were observed and the contribution of medium and large particles was  $> 50\%$ . In early autumn (SF16), despite a significant contribution of medium and large particle classes in the SPM, it can be seen that the share of Chl *a* for these classes was negligible, while ultra and pico particles had the largest contribution.

### New Figure 3

In Figure 3, for all data, it can be seen that the winter season, regardless of the place where POM/SPM samples were taken, assumes the lowest values from SPM. No trends were observed between the remaining seasons and sampling sites. In the case of micro particles, most of the GG samples in autumn are dominated by inorganic particles (POM/SPM < 25%). For nanoparticles, in the winter, inorganic matter dominated, and in the autumn, organic matter dominated. For ultra particles, no seasonal and spatial dependencies of POM/SPM vs SPM are visible. On the other hand, for pico particles, we observed that POM/SPM increases with the increase in SPM: in winter POM/SPM had the lowest values, then in spring and autumn it was on average 65% and the highest values reached in summer on average 80%.

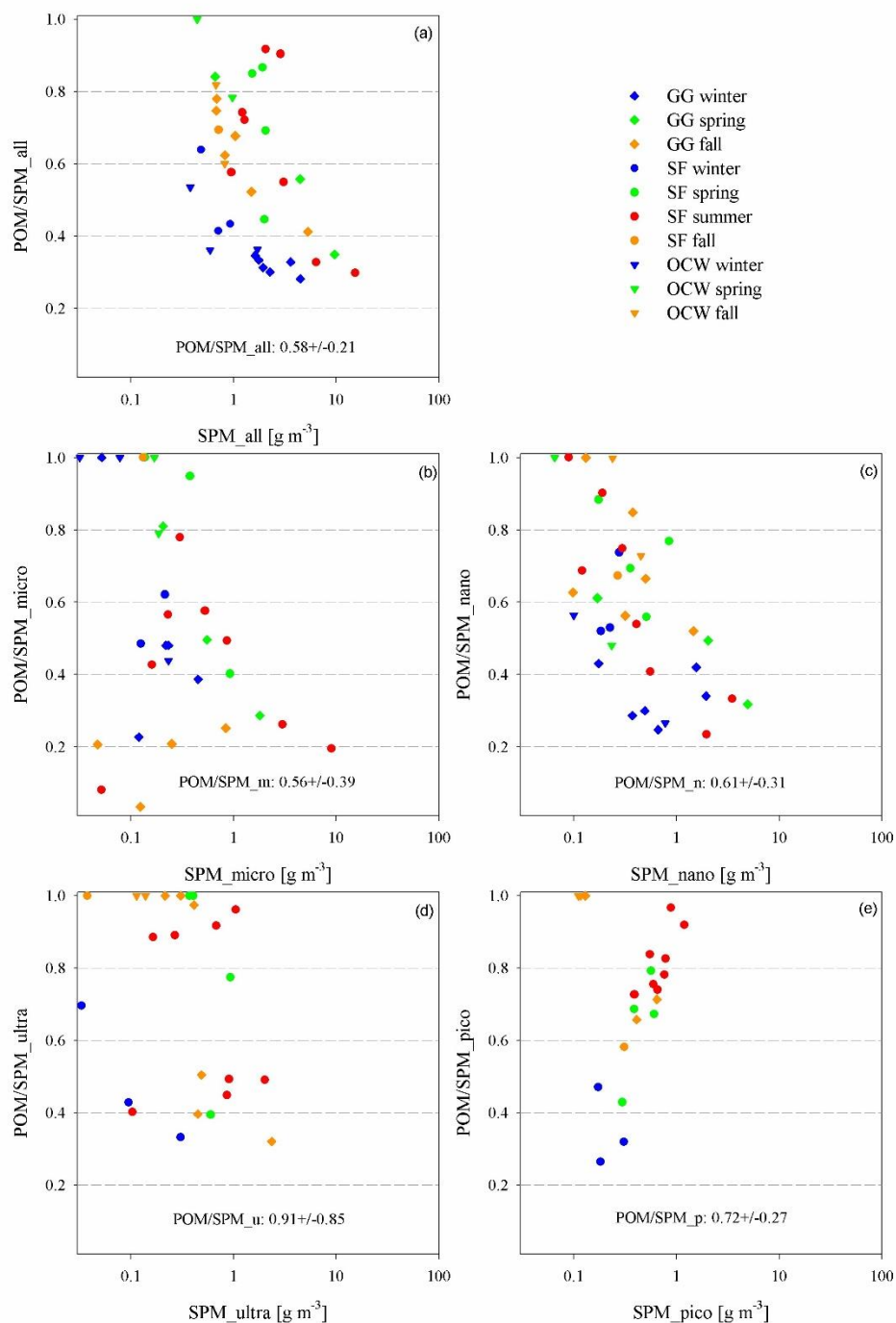


**Figure 3: Relationships between the POM/SPM ratio and the SPM concentration for the original water samples and the size classes: micro, nano, ultra and pico. Mean values  $\pm$  standard deviation are shown in the graph. Markers shapes and colours distinguish the season and sampling site (GG - Gulf of Gdańsk, SF - Sopot Pier, OCW - open and coastal waters).**

New Figure 5

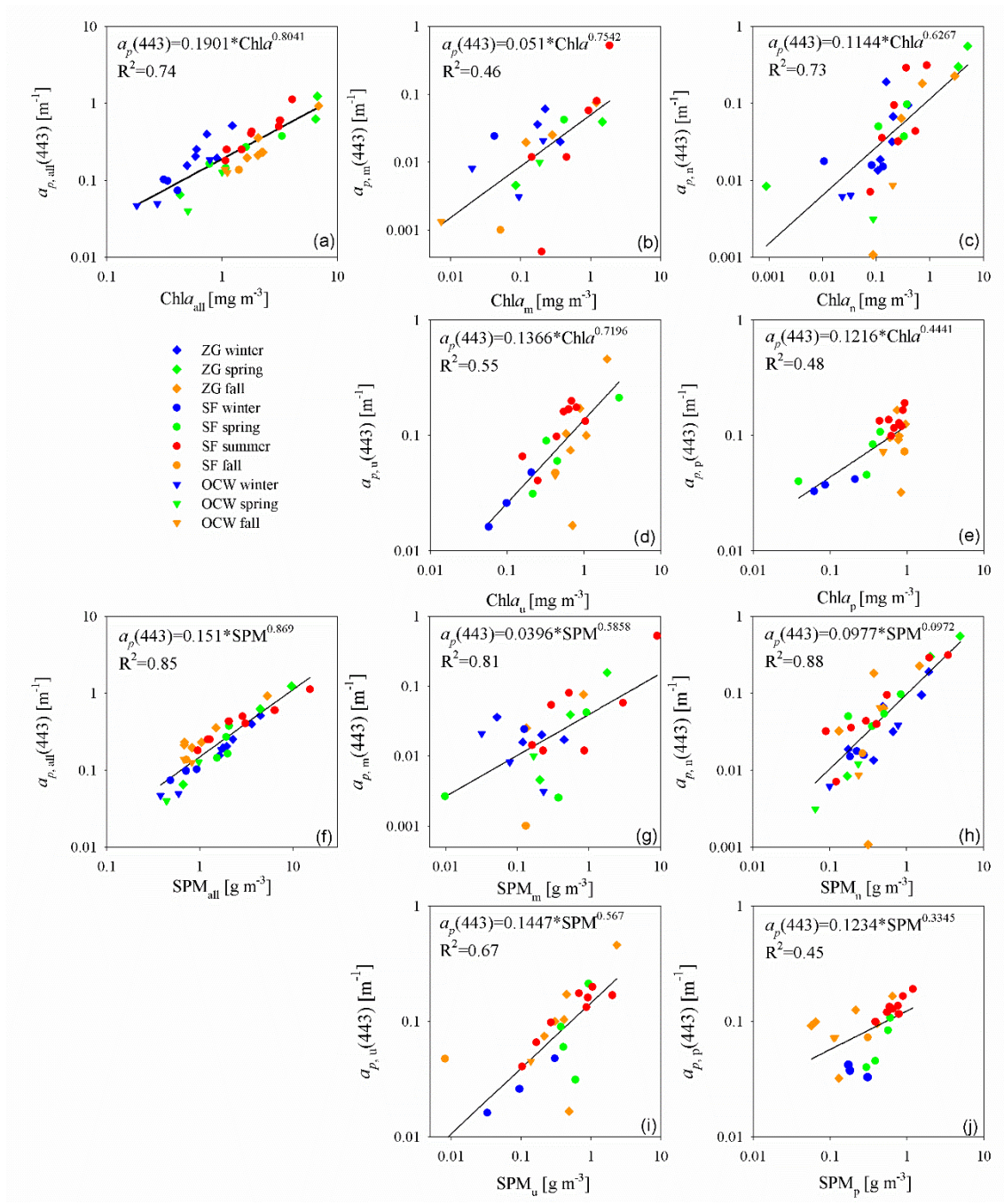


**Figure 5: Relationships of the light absorption coefficients by all unfractionated particles (a, f) and in size classes: micro (b, g), nano (c, h), ultra (d, i) and pico (e, j) from the Chl a (a-e) and SPM (f-j), for the selected wavelength of 443 nm. Note that graphs have different axis scales.**

Figure 5 presents the light absorption coefficients of all particles suspended in seawater for a wavelength of 443 nm depending on the concentration of Chl $a$  and SPM, for the original (unfractionated) seawater samples and for the micro, nano, ultra and pico-size classes in log-log scale. The data was divided due to the season and place of sampling. Approximations are shown for all samples in power form ( $y=Ax^B$ ).

(...)

The relationships  $a_p(443)$  vs Chl $a$  allow to distinguish the winter season from the summer season (blue and red points). In the winter season, the absorption values increase much faster with the increase of Chl $a$  than in other seasons. Taking into account the relationships between  $a_p(443)$  and Chl $a$  in individual size classes, the values are slightly dispersed, but there is also a difference between seasons. In the case of dependence on SPM, a division into seasons is also visible. For all particles in the winter and spring season abs coefficients increase slightly faster with increasing SPM than in summer and autumn. Individual size classes also show seasonal trends, however, further research is necessary to draw clear conclusions. As for the sampling area, as expected, OCW are characterized by lower concentrations of Chl $a$  and SPM than GG, and the related lower values of absorption coefficients.

#### New Figure 6

The Baltic Sea is characterized by a large influence of anthropogenic factors on the optical properties of its waters, including the inflow of a large amount of dissolved and suspended organic substances with river waters into its catchment area (especially the Gulf of Gdańsk, which is strongly influenced by the waters of the Vistula). These are waters with complex optical properties that do not depend solely on Chl $a$ , especially in the case of detritus. However, in order to compare, we showed how  $a_d$  vs Chl $a$  dependencies look like. (...)

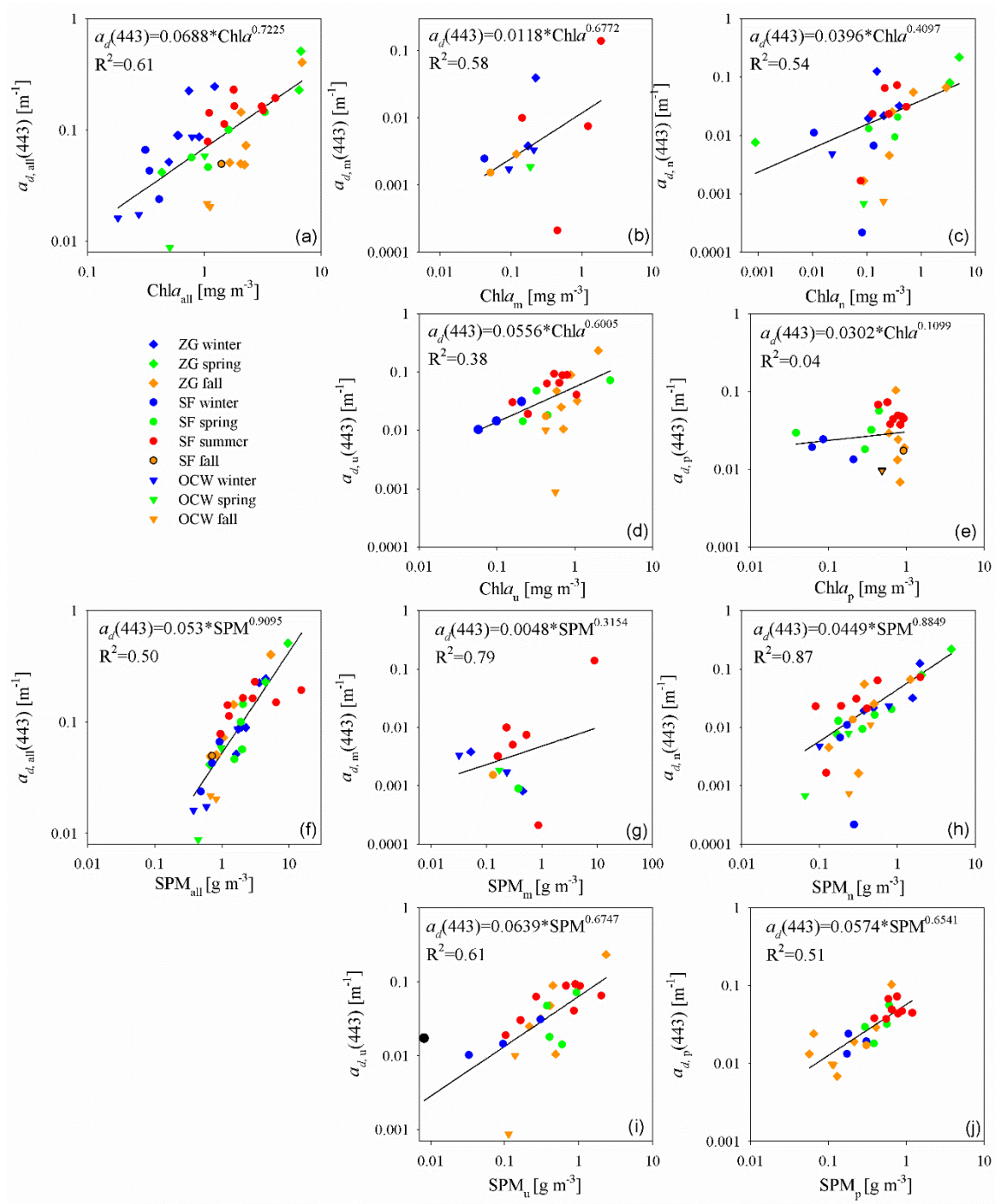


**Figure 6: Relationships of the light absorption coefficients by all unfractionated detritus (a, f) and in size classes: micro (b, g), nano (c, h), ultra (d, i) and pico (e, j) from the Chl *a* (a-e) and SPM (f-j), for the selected wavelength of 443 nm. Note that graphs have different axis scales.**

New Figure 7

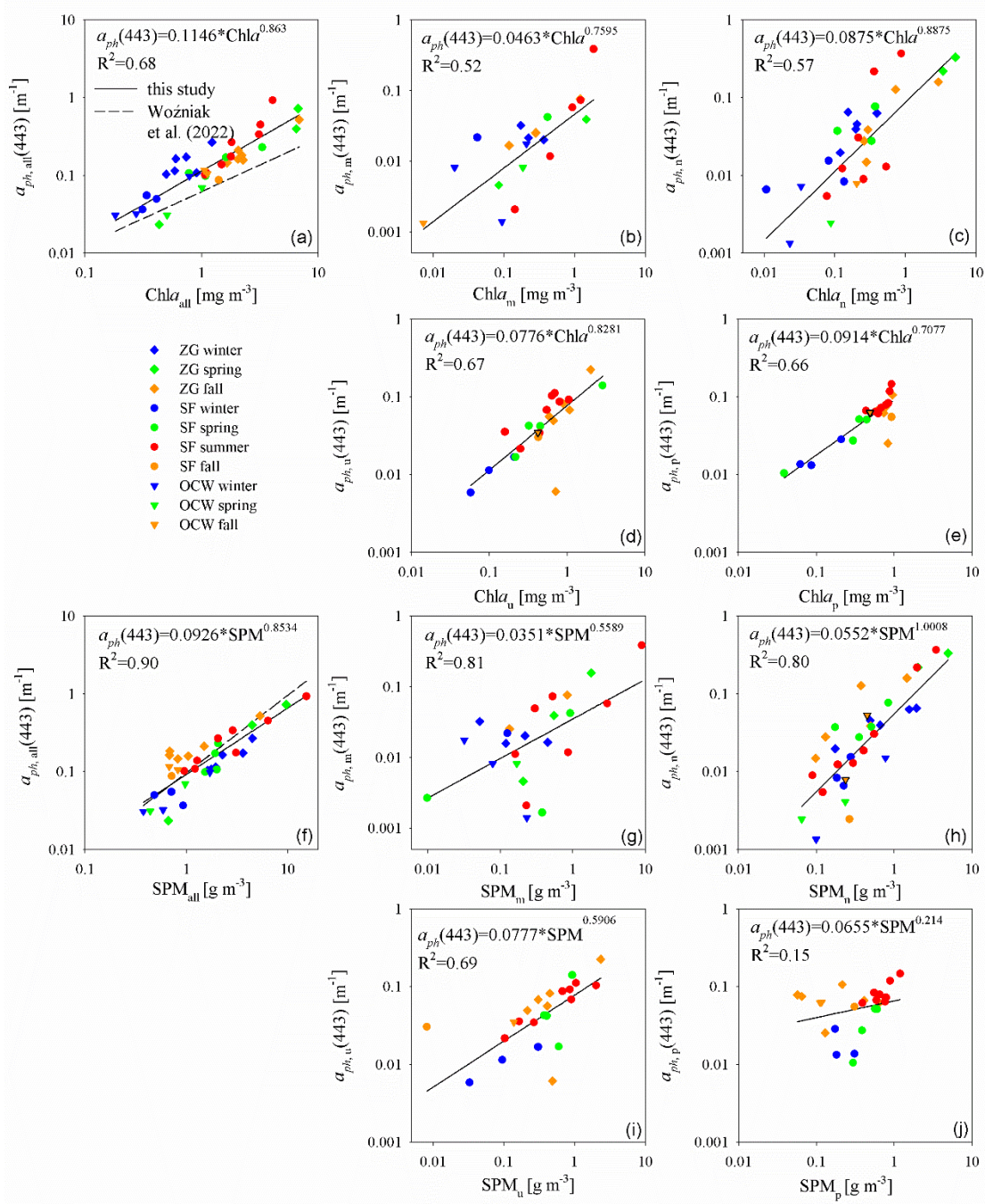


**Figure 7: Relationships of the light absorption coefficients by all unfractionated phytoplankton (a, f) and in size classes: micro (b, g), nano (c, h), ultra (d, i) and pico (e, j) from the Chl  $a$  (a-e) and SPM (f-j), for the selected wavelength of 443 nm. Note that graphs have different axis scales.**

As in the case of light absorption by all particles, seasonal variation can be observed, both for Chl  $a$  and SPM dependence. The winter season is characterized by low Chl  $a$  values and relatively low  $a_{ph}(443)$ . The spring season is characterized by the greatest range of Chl  $a$  variability. Summer and autumn are characterized by Chl  $a$  values  $>1$  and  $a_{ph}(443)$  values highest in a year. Similar trends are visible in the case of division into size classes, with a large

sample dispersion for micro particles. The dependence of  $a_{ph}(443)$  on SPM is characterized by a high coefficient of determination  $R^2 = 0.9$ . We can distinguish the winter and spring seasons, which in most cases lie under the approximation curve, while the data collected in the summer and autumn seasons lie above this curve (see Figure 7).

Reviewer's comments:

*Although average Chl a-specific absorption coefficients of phytoplankton generally decrease with increasing cell size because of self-shading, the authors showed the opposite trends as compared with previous work of Ciotti et al. (2002). Therefore, I feel that the package effect (as mentioned by the authors themselves in Line 410) may be open to further discussion.*

Author's response:

Figure 9 and 10 shows the average spectra of specific light absorption coefficients by all particles, detritus and phytoplankton for given fractions, determined for cases where a given size fraction was dominant (it is not an average for all measured coefficients for a given fraction). In the analyses, we used Chl a determined by spectrophotometry, not by HPLC, so we do not know the share of individual pigment groups, so we are unable to determine the packing effect. Of course, taking into account that the largest share of micro particles was recorded for the SF13 station during phytoplankton bloom (large algae gathered at the beach in Sopot), we can assume that the packing effect occurred and was significant.

Reviewer's comments:

***Minor Comments:***

*Names of observed stations are missing in Figures 1, which make it difficult to refer to Figures 2 and 8 and SF04 and SF13 in Lines 417 – 427. The information will help readers understand the results more easily.*

Author's response:

SF01-SF16 refer to measurements on Sopot Pier and constitute a separate group showing temporal variability. We have improved the descriptions in the text. Figure 1 has been modified, station names have been added.

## New Figure 1

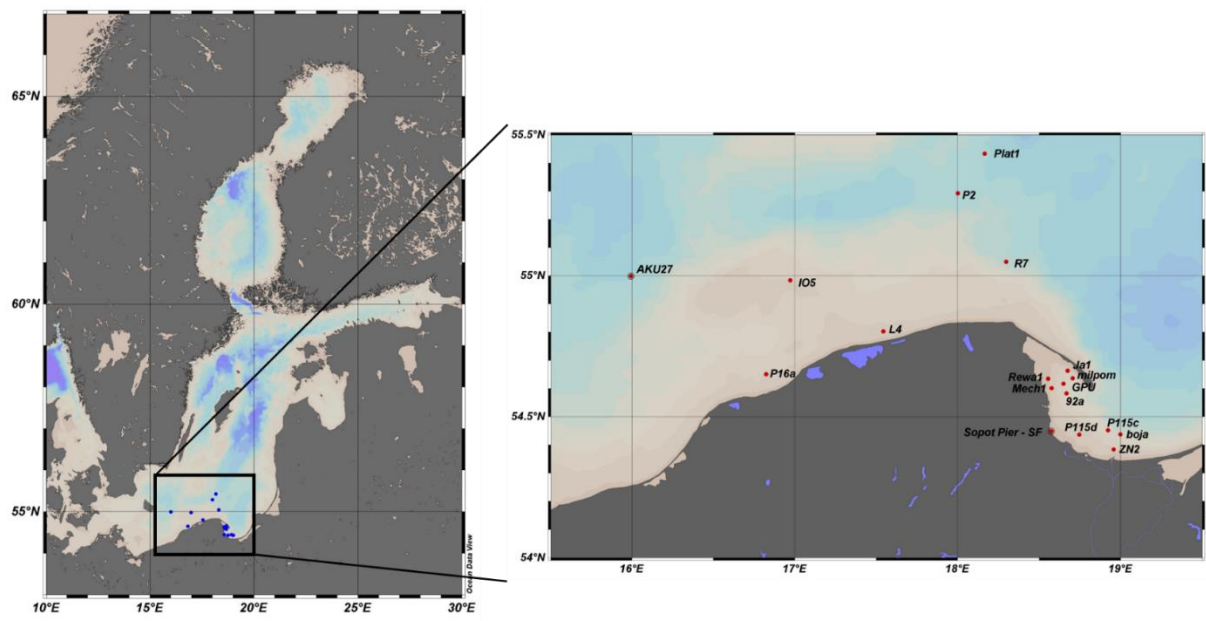


**Figure 1: Location of measurement stations in the Baltic Sea.**

Reviewer's comments:

*I would suggest that the results of Figure 4, 9, or 10 be presented in a different way; for example, a box plot at satellite ocean colour bands with average spectra could be used. I think that this make it easier for the readers to understand the importance of them. For example, please refer to Brunelle et al. (2012, doi: 10.1029/2011JC007345).*

Author's response:

We have presented Figure 4 as suggested by the Reviewer, as far as possible. However, Figures 9 and 10 in boxed form for selected wavelengths do not work in our case. The variability ranges of individual means and standard deviations for size classes overlap, obscuring the picture. Therefore, in the existing drawings, we have bolded the average values for better visibility, and in the Table 4 we have compiled numerical values for selected wavelengths, corresponding to the ranges observed by satellite sensors such as Seawifs or OLCI.

New Figure 4

Figure 4 shows the spectra of light absorption coefficients for all suspended particles, detritus, and phytoplankton determined in the analyzed dataset. The left panel (Figure 4a, c, e) shows the variability of these coefficients for the original unfractionated seawater samples. For an analyzed data sat variability of two orders of magnitude was recorded. The bold line shows the average absorption spectra. The range of variation of absorption coefficients for selected wavelengths is shown in the form of boxes with whiskers. The boxes show the data set between the 25th and 75th percentiles, while the whiskers indicate the 10th and 90th percentiles. Points outside the whiskers are outliers. The line in the boxes indicates the median. The selected wavelengths correspond to the mid-wavelengths of the bands observed by the OLCI (Ocean and Land Colour Instrument) sensor on the Sentinel satellite. The right

panel of Figure 4 (b, d, f) shows the variability of  $a_p(\lambda)$ ,  $a_d(\lambda)$  and  $a_{ph}(\lambda)$ , calculated for the micro, nano, ultra and pico-size classes. Bold lines are average spectra in a given size class, thin dashed lines show the range of variability (min-max). The variability was greater than two orders of magnitude, whereas for the pico class it was one order of magnitude.

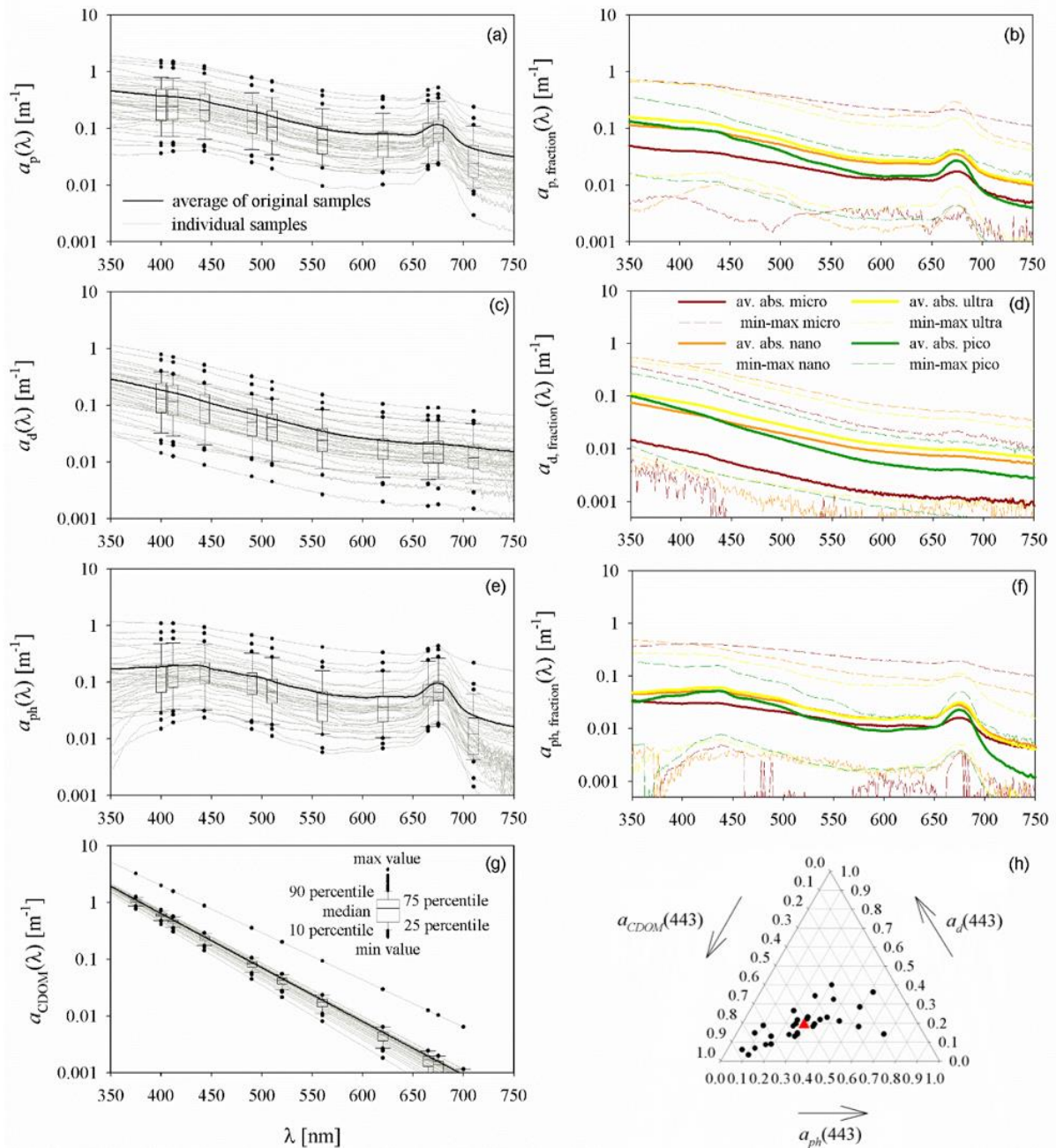


**Figure 4: Spectra of light absorption coefficients by particles suspended in seawater ( $a_p(\lambda)$ ), detritus ( $a_d(\lambda)$ ) and phytoplankton ( $a_{ph}(\lambda)$ ) for original, unfractionated water samples - left panel (a, c, e) and calculated for micro, nano, ultra and pico-size classes - right panel (b, d, f); spectra of CDOM light absorption coefficients ( $a_{CDOM}(\lambda)$ ) (g) and ternary plot showing the light absorption budget for the 443 nm wavelength in the analyzed dataset (h) (the red triangle shows the average contribution of individual absorption coefficients to the total light absorption).**

New Figure 9

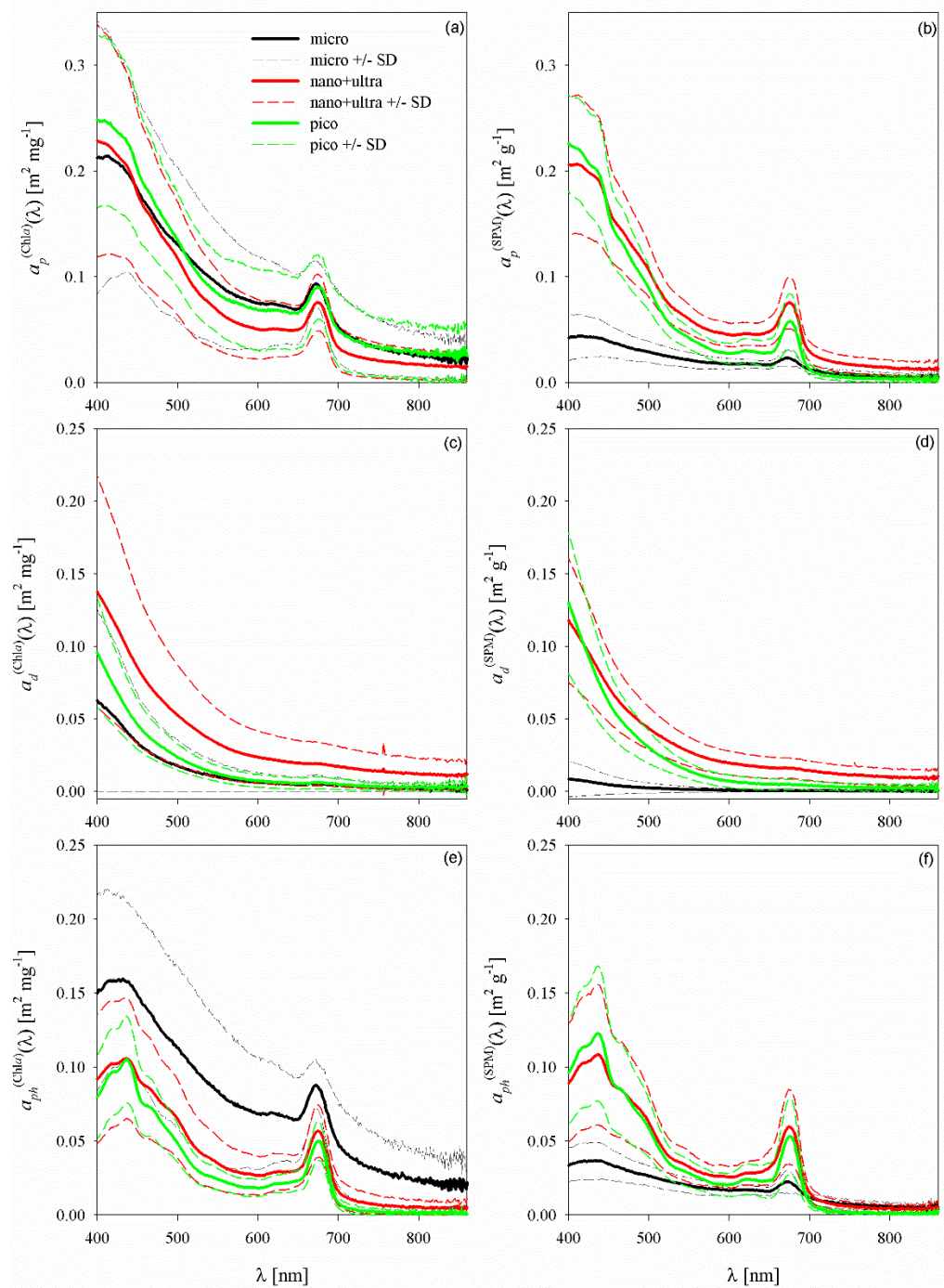


**Figure 9: Mean chlorophyll-specific (left panel) and mass-specific (right panel) light absorption coefficients for all particles (a, b), detritus (c, d) and phytoplankton (e, f) for 3 size classes : micro-, nano+ultra- and picoplankton. SD means standard deviation.**

New Figure 10

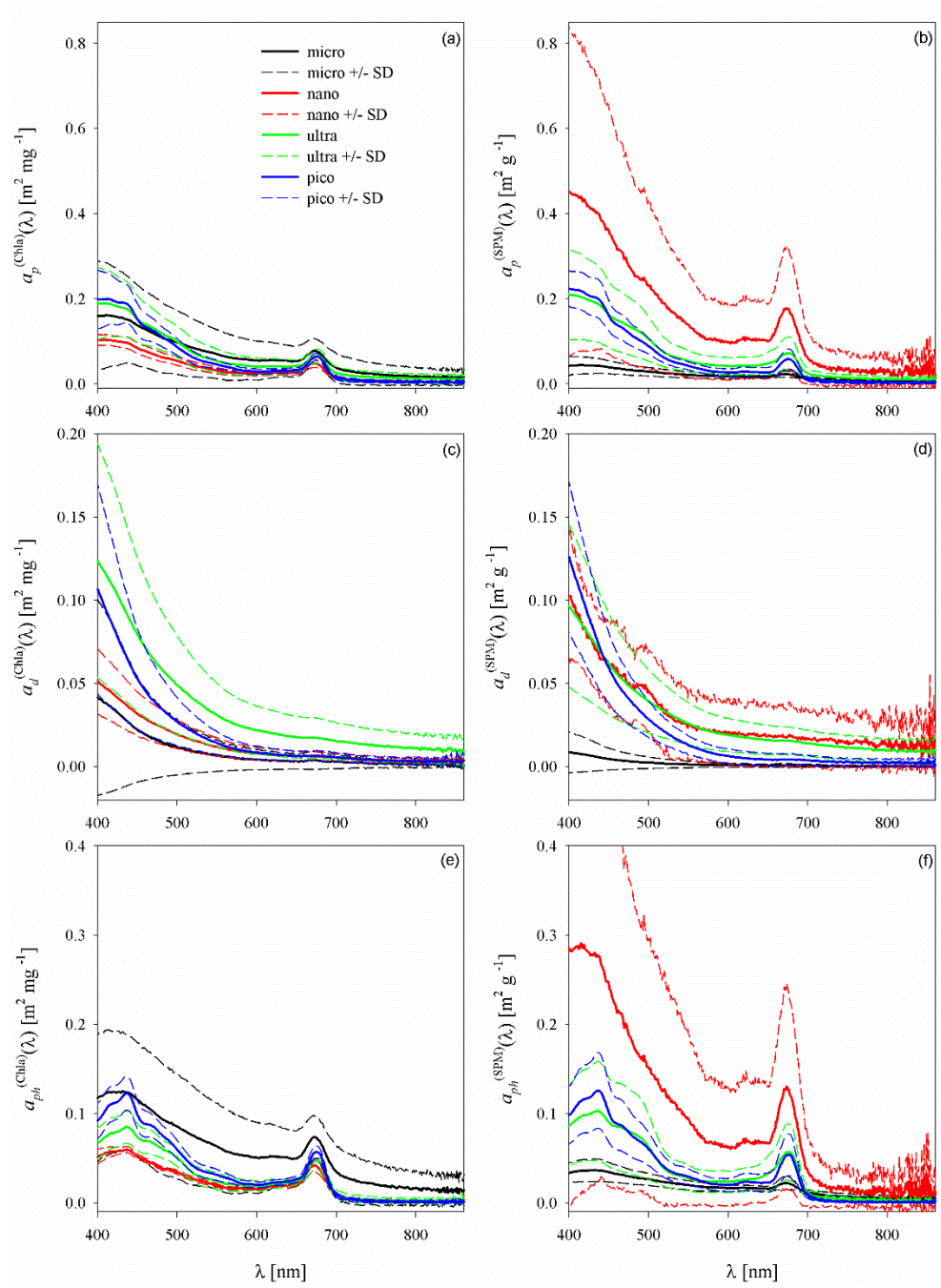


**Figure 10: Mean chlorophyll-specific (left panel) and mass-specific (right panel) light absorption coefficients for all particles (a, b), detritus (c, d) and phytoplankton (e, f) for 4 size classes : micro-, nano-, ultra- and picoplankton. SD means standard deviation.**

New Table 4

**Table 4: Average values of chlorophyll-specific and mass-specific light absorption coefficients for all particles, detritus and phytoplankton calculated for a given size class with standard deviations for selected wavelengths corresponding to selected bands of the OLCI sensor.**

	400 nm	443 nm	510 nm	620 nm	675 nm	709 nm
$\alpha_{p,micro}^{(Chla)}(\lambda)$	0.160+/- 0.135	0.147+/- 0.098	0.091+/- 0.072	0.056+/- 0.041	0.077+/- 0.028	0.033+/- 0.032
$\alpha_{p,nano}^{(Chla)}(\lambda)$	0.104+/- 0.013	0.092+/- 0.013	0.048+/- 0.010	0.027+/- 0.006	0.048+/- 0.009	0.011+/- 0.004
$\alpha_{p,ultra}^{(Chla)}(\lambda)$	0.190+/- 0.085	0.167+/- 0.061	0.086+/- 0.035	0.041+/- 0.018	0.066+/- 0.016	0.021+/- 0.015
$\alpha_{p,nano+ultra}^{(Chla)}(\lambda)$	0.229+/- 0.110	0.195+/- 0.083	0.103+/- 0.050	0.051+/- 0.027	0.076+/- 0.027	0.029+/- 0.020
$\alpha_{p,pico}^{(Chla)}(\lambda)$	0.244+/- 0.055	0.199+/- 0.038	0.082+/- 0.018	0.031+/- 0.004	0.061+/- 0.007	0.011+/- 0.004
$\alpha_{d,micro}^{(Chla)}(\lambda)$	0.042+/- 0.058	0.025+/- 0.035	0.010+/- 0.015	0.004+/- 0.006	0.004+/- 0.006	0.003+/- 0.004
$\alpha_{d,nano}^{(Chla)}(\lambda)$	0.052+/- 0.032	0.035+/- 0.014	0.018+/- 0.008	0.007+/- 0.003	0.006+/- 0.003	0.005+/- 0.002
$\alpha_{d,ultra}^{(Chla)}(\lambda)$	0.124+/- 0.070	0.086+/- 0.050	0.045+/- 0.027	0.020+/- 0.014	0.018+/- 0.012	0.015+/- 0.011
$\alpha_{d,nano+ultra}^{(Chla)}(\lambda)$	0.138+/- 0.080	0.093+/- 0.056	0.048+/- 0.032	0.021+/- 0.017	0.019+/- 0.015	0.017+/- 0.014
$\alpha_{d,pico}^{(Chla)}(\lambda)$	0.155+/- 0.044	0.085+/- 0.027	0.032+/- 0.010	0.008+/- 0.004	0.006+/- 0.003	0.005+/- 0.003
$\alpha_{ph,micro}^{(Chla)}(\lambda)$	0.118+/- 0.071	0.122+/- 0.064	0.081+/- 0.058	0.052+/- 0.036	0.073+/- 0.023	0.030+/- 0.028
$\alpha_{ph,nano}^{(Chla)}(\lambda)$	0.052+/- 0.008	0.057+/- 0.003	0.031+/- 0.003	0.019+/- 0.002	0.041+/- 0.0074	0.006+/- 0.002
$\alpha_{ph,ultra}^{(Chla)}(\lambda)$	0.067+/- 0.017	0.081+/- 0.018	0.042+/- 0.001	0.021+/- 0.005	0.048+/- 0.010	0.007+/- 0.002
$\alpha_{ph,nano+ultra}^{(Chla)}(\lambda)$	0.092+/- 0.044	0.102+/- 0.039	0.055+/- 0.024	0.029+/- 0.013	0.057+/- 0.018	0.012+/- 0.009
$\alpha_{ph,pico}^{(Chla)}(\lambda)$	0.089+/- 0.019	0.114+/- 0.019	0.049+/- 0.011	0.023+/- 0.002	0.055+/- 0.006	0.006+/- 0.002
$\alpha_{p,micro}^{(SPM)}(\lambda)$	0.054+/- 0.017	0.052+/- 0.007	0.032+/- 0.008	0.020+/- 0.004	0.028+/- 0.004	0.011+/- 0.005
$\alpha_{p,nano}^{(SPM)}(\lambda)$	0.453+/- 0.385	0.380+/- 0.300	0.212+/- 0.180	0.107+/- 0.094	0.176+/- 0.140	0.050+/- 0.050
$\alpha_{p,ultra}^{(SPM)}(\lambda)$	0.210+/- 0.107	0.178+/- 0.086	0.089+/- 0.042	0.043+/- 0.021	0.072+/- 0.038	0.021+/- 0.009
$\alpha_{p,nano+ultra}^{(SPM)}(\lambda)$	0.0189+/- 0.160	0.152+/- 0.113	0.086+/- 0.070	0.045+/- 0.038	0.057+/- 0.035	0.028+/- 0.028
$\alpha_{p,pico}^{(SPM)}(\lambda)$	0.227+/- 0.046	0.185+/- 0.047	0.074+/- 0.017	0.030+/- 0.011	0.058+/- 0.026	0.009+/- 0.004
$\alpha_{d,micro}^{(SPM)}(\lambda)$	0.026	0.016	0.007	0.003	0.003	0.002
$\alpha_{d,nano}^{(SPM)}(\lambda)$	0.144+/- 0.022	0.090+/- 0.016	0.061+/- 0.031	0.028+/- 0.028	0.029+/- 0.029	0.026+/- 0.026

$\sigma_{d,ultra}^{(SPM)} (\lambda)$	0.090+/- 0.049	0.067+/- 0.033	0.036+/- 0.017	0.018+/- 0.009	0.016+/- 0.008	0.014+/- 0.008
$\sigma_{d,nan+ultra}^{(SPM)} (\lambda)$	0.108+/- 0.099	0.072+/- 0.066	0.039+/- 0.038	0.019+/- 0.020	0.017+/- 0.018	0.015+/- 0.016
$\sigma_{d,pico}^{(SPM)} (\lambda)$	0.130+/- 0.048	0.069+/- 0.026	0.026+/- 0.009	0.006+/- 0.004	0.005+/- 0.004	0.004+/- 0.003
$\sigma_{ph,micro}^{(SPM)} (\lambda)$	0.041+/- 0.004	0.045+/- 0.001	0.028+/- 0.005	0.019+/- 0.003	0.027+/- 0.005	0.063+/- 0.005
$\sigma_{ph,nano}^{(SPM)} (\lambda)$	0.381+/- 0.313	0.335+/- 0.257	0.182+/- 0.152	0.093+/- 0.078	0.161+/- 0.120	0.037+/- 0.029
$\sigma_{ph,ultra}^{(SPM)} (\lambda)$	0.086+/- 0.045	0.099+/- 0.054	0.050+/- 0.027	0.026+/- 0.013	0.057+/- 0.032	0.008+/- 0.005
$\sigma_{ph,nano+ultra}^{(SPM)} (\lambda)$	0.088+/- 0.071	0.085+/- 0.055	0.050+/- 0.036	0.027+/- 0.021	0.042+/- 0.020	0.014+/- 0.014
$\sigma_{ph,pico}^{(SPM)} (\lambda)$	0.096+/- 0.035	0.116+/- 0.043	0.047+/- 0.016	0.024+/- 0.010	0.053+/- 0.026	0.005+/- 0.002